doi:10.1017/S143192762001524X
Microsc. Microanal. 26 (Suppl 2), 2020
© Microscopy Society of America 2020

Binucleate Cell Atlasing: An Intracellular Object Localization Tool for Single-Cell Fluorescence Microscopy

Andrew Soltisz, Rengasayee Veeraraghavan and Seth Weinberg

The Ohio State University, Columbus, Ohio, United States

Cardiomyocytes are a relatively large, binucleated, polarized cell type whose membranes feature multiscale spatial domains. There, the location and organization of proteins, such as ion channels or mechanical junction proteins, greatly affect cardiac conduction[1-4] and excitation-contraction coupling[5-8]. The ability to describe the location of these membranous or cytosolic objects within the cell has significant utility for bridging the gap between cell structure and function. However, the methods to do so thus far remain largely qualitative or lack descriptive power, preventing robust statistical analysis. Morphological heterogeneity between cells also creates a critical barrier to statistical analysis that precludes direct comparison of image data across multiple cells. Here, we present a quantitative technique for localizing intracellular objects in binucleate cells based on the position of the objects relative to both nuclei and the cell periphery. This method is applicable to any 2- or 3-dimensional (2D or 3D) single cell image of fluorescent signal and therefore can be extended to collate data acquired using multiple imaging modalities. The binucleate nature of cardiomyocytes provides an easy yet highly informative means for localizing intracellular objects. Using the two nuclei as fiducial markers, the entire body of the cell can be spatially atlased to provide a means for cell-morphology-agnostic object localization. For a given cell, the nuclear stain image is used to generate a mask of the cell nuclei. The raw nuclear image is first processed by applying an intensity threshold to the grey-scale image to remove low intensity pixels, creating a binary image. Then a small-kernelled morphological closing filter is applied to fill any holes in the nuclei. The nuclei are then segmented by only keeping the two largest objects from the connected components of the image using a connectivity of 8 or 26 for 2- or 3-D images respectively. The object-stained images are also processed with an intensity threshold to remove noise and binarize the image. Finally, every pixel from the object channel is indexed, their spatial coordinates within the image are calculated, and their distances to both nuclear centroids calculated. These distance measurements are then used to generate a bivariate histogram where the x-coordinate of a pixel corresponds to the smaller of the two nuclear distances, the y-coordinate corresponds to the larger of the two nuclear distances, and the z-axis or heat-map color corresponds to the count or fraction of pixels with a particular x-y pair (Figure 1A). All x-y coordinates on the bivariate histogram directly map onto a region of the cell as diagrammed by figure 1B. The lines and points that define and segment the available histogram data space are functions of the cell geometry that can be derived from either the distance between nuclear centroids or by plotting the nuclear distances of all intracellular pixels, thus providing a means to atlas the intracellular space. Future work aims to apply this technique to multiple imaging modalities including confocal immunofluorescence, proximity ligation assays, and STORM super-resolution microscopy.

https://doi.org/10.1017/S143192762001524X Published online by Cambridge University Press

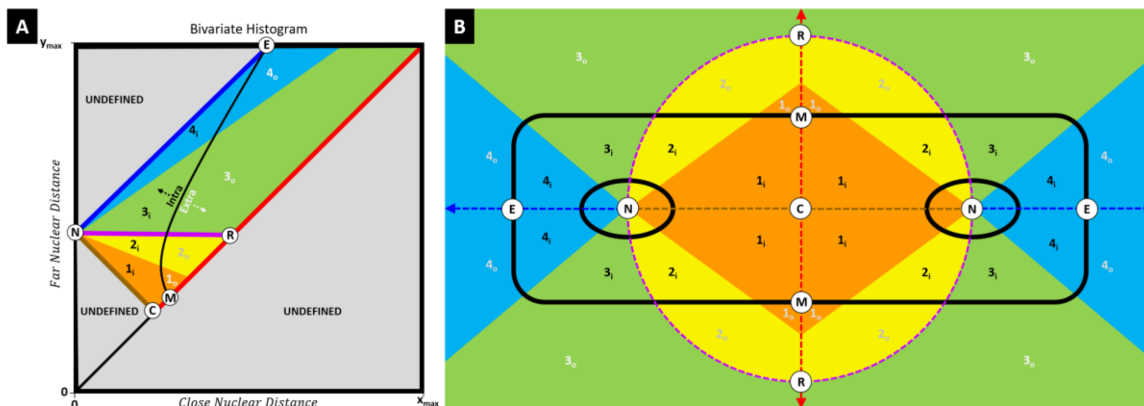

Figure 1. Diagram showing how pixels composing the binucleate cell body map onto the bivariate histogram. (A) The histogram can be divided into distinct and explicitly defined regions: All data histogram points must fall above the line of identity, as the close nuclear distance (x) will always be smaller than the far nuclear distance (y). This creates a triangle of undefined space at the bottom right corner of the histogram below the line of identity. Another triangle of undefined space located at the bottom left corner of the histogram is defined by points C, N, and the origin. Point C is defined by the coordinates (d/2,d/2), where d is the distance between the two nuclear centroids, and point N is defined by the coordinates (0,d). A third triangle of undefined space located at the top left corner of the histogram is defined by points N, E, and (0,ymax), where E is defined by the coordinates (xmax - d,ymax). All histogram points that fall below the purple line map onto the cell region that lies between the nuclei (yellow and orange cell regions), and all histogram points above the purple line map onto the region at the ends of the cell (green and blue cell regions). The purple histogram line is defined by the points N and R, where point R is defined by the coordinates (R,R). The brown and blue histogram lines indicate pixels that map onto the longitudinal midline of the cell, where the brown line runs medially between the nuclei and the blue line continues laterally past each nucleus towards the ends of the cell. The red histogram line maps onto the lateral midline of the cell. The black histogram curve that spans from point M to point E roughly indicates pixels that map onto the cell's periphery, where all points above and left of the line indicate intracellular pixels, and all points below and right of the line indicate extracellular pixels. Point M maps to the pixels on the cell where the lateral midline (red line) intersects the cell periphery. (B) Every line, point, and colored region of the bivariate histogram maps onto the 2- or 3-D cell body.

References

1. Veeraraghavan R and Gourdie R. Stochastic Optical Reconstruction Microscopy-based Relative Localization Analysis (STORM-RLA) for Quantitative Nanoscale Assessment of Spatial Protein Organization. Molecular biology of the cell. 2016;27:3583-3590.
2. Veeraraghavan R, Hoeker GS, et al. The adhesion function of the sodium channel beta subunit (beta1) contributes to cardiac action potential propagation. Elife. 2018;7.
3. Veeraraghavan R, Lin J, et al. Sodium channels in the Cx43 gap junction perinexus may constitute a cardiac ephapse: an experimental and modeling study. Pflugers Arch. 2015;467:2093-2105.
4. Veeraraghavan R, Lin J, et al. Potassium channels in the Cx43 gap junction perinexus modulate ephaptic coupling: an experimental and modeling study. Pflugers Arch. 2016;468:1651-61.
5. Radwanski PB, Brunello L, et al. Neuronal Na+ channel blockade suppresses arrhythmogenic diastolic Ca2+ release. Cardiovascular research. 2015;106:143-52.

https://doi.org/10.1017/S143192762001524X Published online by Cambridge University Press

6. Radwański PB, Ho H-T, et al. Neuronal Na+ Channels Are Integral Components of Pro-Arrhythmic Na+/Ca2+ Signaling Nanodomain That Promotes Cardiac Arrhythmias During β-Adrenergic Stimulation. JACC: Basic to Translational Science. 2016;1:251-266.
7. Struckman HL, Baine S, et al. Super-Resolution Imaging Using a Novel High-Fidelity Antibody Reveals Close Association of the Neuronal Sodium Channel NaV1.6 with Ryanodine Receptors in Cardiac Muscle. Microsc Microanal. 2020:1-9.
8. Koleske M, Bonilla I, et al. Tetrodotoxin-sensitive Navs contribute to early and delayed afterdepolarizations in long QT arrhythmia models. The Journal of general physiology. 2018.

https://doi.org/10.1017/S143192762001524X Published online by Cambridge University Press